Crane Girder Deformation Mapping Using Image Processing and Template Matching of Laser Scanner Point Cloud

Authors

S. Deshpande
Associate Professor, Pennsylvania State University, Wilkes-Barre, Pa., USA

M. Falk (pictured)
President/Chief Executive Officer, Falk-PLI Engineering and Surveying, Portage, Ind., USA
mfalk@falk-pli.com

N. Plooster
Director of Surveying, Falk-PLI Engineering and Surveying, Portage, Ind., USA
nplooster@falk-pli.com

Repetitive loading of factory crane girders causes deformation and/or failure. In the presented method, light detection and ranging points over one face of a girder are processed to create deformation maps of panels: web area between stiffeners and flanges. Web surface profiles at top, mid and bottom locations are created by matching a standard I-section template to point data. Root mean square error (RMSE) at each girder slice is computed by comparing the nearest girder points and inflection points from the template. The girder point with the lowest RMSE is selected as the correct match and three locations are identified.

Overhead gantry cranes are an integral part of a steel mill. Fig. 1 shows a schematic diagram of a gantry crane and its different components. These cranes operate on rails supported by girders. The girders are supported by columns that transfer the load to the foundation. Due to recurring use of the overhead cranes, stresses are created in all the supporting structural members that could result in deformations. Such deformations could be difficult to detect by visual inspection. If unaddressed, these deformations could result in accidents causing loss of life and/or property. Therefore, manual inspection of these structural members using tactile tools is necessary for the smooth functioning of any facility.

The length of a typical crane girder could extend to thousands of feet. Manual inspection of structural members can be time-consuming and lack details. Any downtime for inspection, repair and maintenance could result in significant time and revenue losses. Therefore, it is necessary to develop methodologies that could expedite inspection without any downtime for the crane. In recent years, laser scanning technology has been used to determine structural deformations, but manual extraction of features from large three-dimensional (3D) point data set can be time-consuming and could be influenced by operator's judgment. Additionally, complete utilization of the data would not be possible by manual extraction of pertinent information from laser point data set.

This paper presents a new methodology to determine crane girder deformations by analyzing laser scanner data. The main objectives are to determine deformations by minimum human interactions, maximize the use of laser point cloud and save time by automation.

Background Information

Laser Scanning – Laser point cloud can be acquired using light detection and ranging (lidar) technology. This technology has significantly evolved in recent decades. Lidar sensors can be mounted on mobile platforms such as cars or trains,[1–3] aerial platforms,[4] or on a tripod.[5] The platforms are selected depending on the purpose of scanning. The basic principle of a laser scanner is based on calculating the time taken by a light pulse to travel from the sensor to an object and back to the sensor.[6]

In recent decades, aerial lidar has been extensively used in various civil engineering applications.[6–10] Mobile mapping lidar is now being used widely for monitoring various transportation applications. The use of terrestrial scanner has also increased in numerous fields such as architecture, construction

management and archeological mapping. The increased use of lidar in various applications can be attributed to the high-point density of lidar sensor and its improved accuracy over the past decade.

Use of Terrestrial Laser Scanning — Lidar scanners are increasingly being used in indoor mapping applications. Laser scanners are also being used to model the deformation of structural members. Selvaraj et al.[11] presented a 3D non-contact laser-scanning method to quantify the deviations in cold-formed steel channel sections (plain and lipped). Their methodologies to segregate the different categories of imperfections from the deviations in the geometry of C-section member were presented. Their methodologies modeled the steel members by their major and minor axis. Cabaleiro et al.[12] presented an approach for 3D modeling of beams in structures using laser scanning. A novel algorithm was developed that performed the segmentation of a beam point cloud based on digital image processing. A polynomial surface, fitting of flange points was performed to model the deformations of beams based on the combined effects of bending moment and torsions deflections. The product was a 3D model of the deformed beam.

A novel approach of extraction and determining roller deformation in steel mills was reported by Deshpande et. al.[5] This method was semi-automated and extracted pertinent measurements from the point cloud. However, the use of laser scanners in the steel industry is not prevalent. Manual extraction of information from the point cloud further hinders the optimum use of the amount of information available in the point cloud. Based on the status of the research in the field of laser scanning in the steel manufacturing industry, this paper proposes a novel semi-automated method of extracting valuable girder deformation measurements from the point cloud. This method is time efficient and increases the accuracy of the deliverables. Such a methodology can greatly enhance the capabilities of a company to prevent accidents thereby preventing downtime due to repair and maintenance.

Description of Data

The data used in this study was acquired in a steel mill in the United States. A lidar scanner was used to collect points on the girders. A reference frame as shown in Fig. 1 was established where the X-axis was parallel to the centerline of the bay, Y- axis was perpendicular to the girder, and the Z-axis was parallel to the plumb direction. As shown in Fig. 2, the point cloud covered only one face of the girder. It can be noted that due to the scan angle, various point densities were obtained on the web and flange of the girder. The methodology developed to extract different measurements from the point data is explained in the next section.

Figure 1

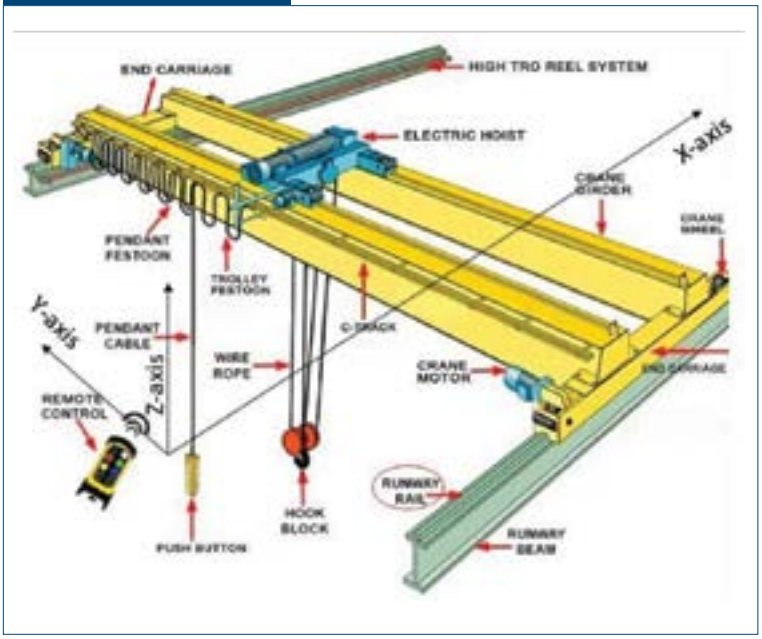

Schematic diagram of a gantry crane showing different components and the 3D reference frame.[1]

Figure 2

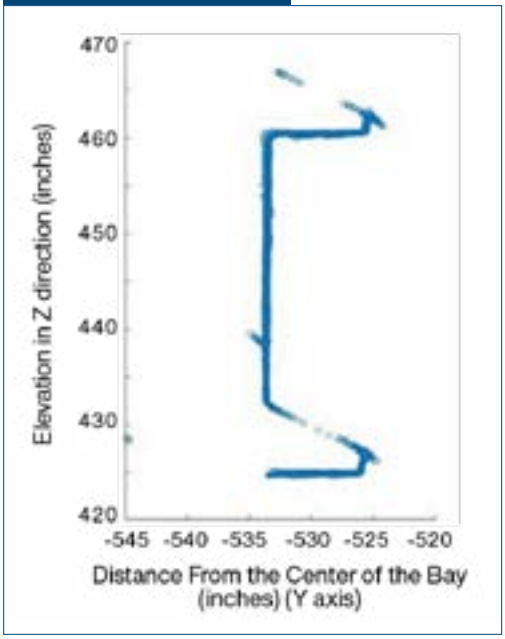

A representative template cross-section of the lidar points on girder.

Methodology

Data Preparation – The methodology was implemented in a Matlab environment. Therefore, the girder data was exported in a text format. As the scanner places points on all objects, it was necessary to eliminate unnecessary data points. A bounding box was defined so that the lidar points on the girder were selected. This step allowed for the elimination of unnecessary data and focused on the girder points.

Overview of the Methodology – The entire methodology can be broadly divided into two parts: color mapping of girder deformation and girder profiles determination by template matching. These two parts are described in the following subsections.

Color Mapping Girder Deformation – The methodology developed for color mapping girder deformation is shown in Fig. 3. The points on the girder were imported in Matlab and were converted to image using interpolation. Fig. 5a shows the grayscale image with a cell size of 0.05 inch. This image was created in the X-Z plane. Image processing steps were implemented as shown in Fig. 5.

First, edges were detected using edge detection.[13] Then the edges were dilated and eroded so that the edges at the panel would merge as a continuous line and the panel region would be empty, without any edges. These panels were detected by clustering pixels and measuring their width and height. Based on a minimum width criterion of 0.5 foot, the panels were validated. Fig. 5b shows the panels identified. At this step, the extents of every panel were determined. Laser points within the extents of each panel were selected and plane fitting was performed. Any deformation within each panel was mapped. Fig. 5c shows the deformation within each panel. Column locations were manually identified as shown in Fig. 5b. The panel points between columns were analyzed and deformations were determined. Fig. 5d shows a color map of panel deformation from column to column.

Girder Deformation Profiles Extraction by Template Matching – Fig. 4 shows the overview of the girder deformation profiles extraction methodology by template matching. Using the standard dimensions of the girder, a template cross-section girder was generated as shown in Fig. 6a.

Critical measurement points (CMPs) were identified at the mid, bottom and top locations along the web face of the template girders. These locations were used to measure points on the surface of the girder. To avoid processing unnecessary data, both the data points were trimmed to include only the girder points. The template was also trimmed to only have points on one side of the girder. Inflection points (IP) as shown were also identified that were later used in the template matching process. The IPs, CMPs points and the trimmed cross-section template points are shown

Figure 3

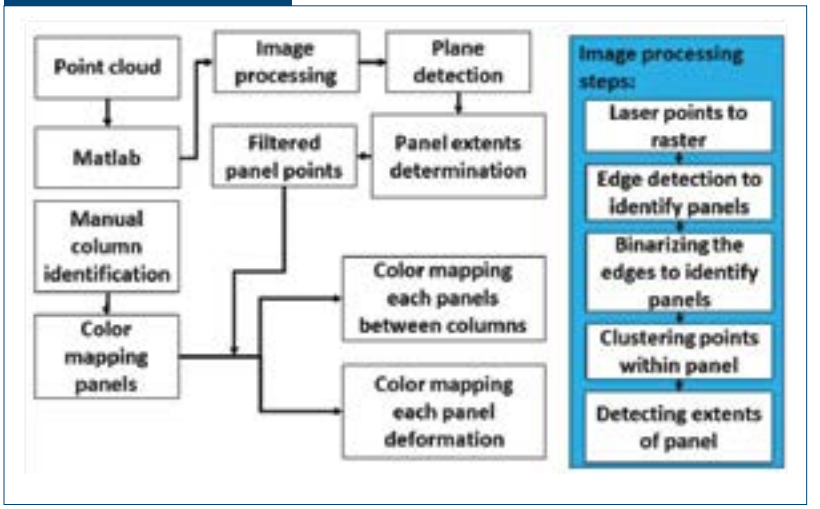

Methodology of color mapping girder deformations.

Figure 4

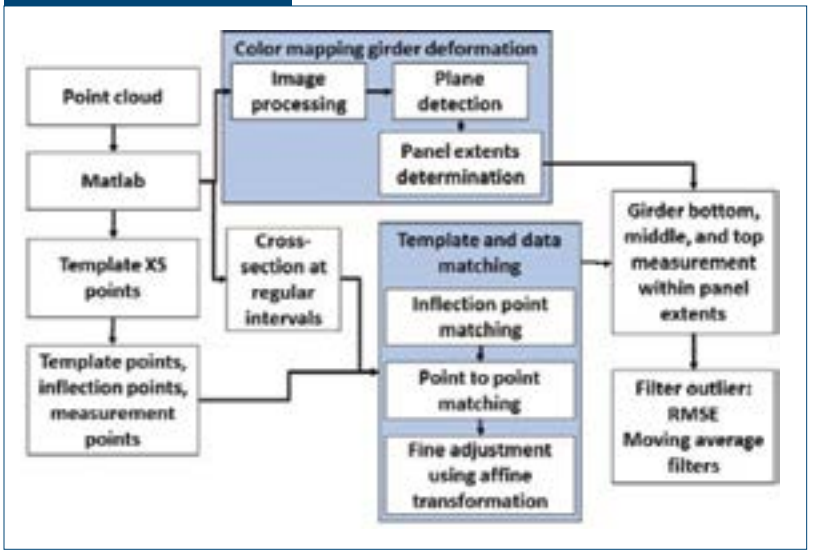

Methodology of girder deformation profiles extraction by template matching.

Figure 5

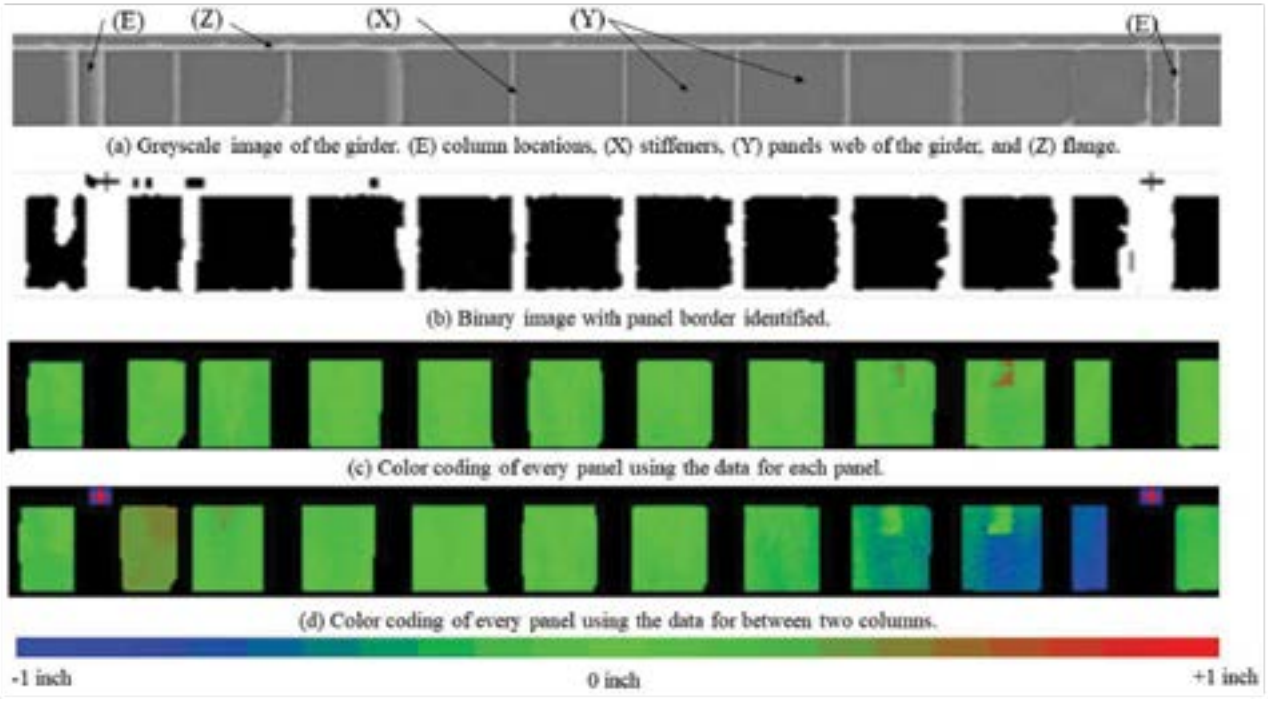

Steps of panel coloring methodology.

Figure 6

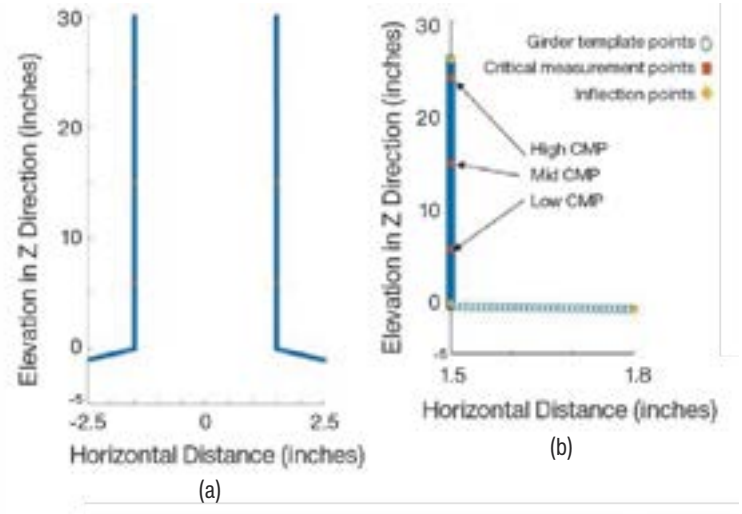

Template points of a standard size girder.

in Fig. 6b. At this stage, the data points in Matlab and the template with the CMPs and IPs were available.

Point-To-Point Matching – The point-to-point matching process involved matching the template points and the data points. This process was implemented in the Y-Z plane that was perpendicular to the length of the girder. The data was processed at every foot starting at one end of the girder to another. The point-to-point matching was performed in three substeps:

Data Point to IP Matching: In this subpart, the set of IPs were translated on every data point using the lowest IP as the reference point. The closest data points to the IPs were determined and Euclidean distances between the IPs and their nearest points were calculated. A sum of these distances was considered as the separation between the IPs and the data points. This process was repeated at all the data points. One percent of data points with the least total separation were shortlisted for the next step.

Dense Data Point to IP Matching: In this subpart, the shortlisted points from the previous steps were used. All template points were compared to the data points to calculate the Euclidean distances between each template and data point. Root mean square error (RMSE) was calculated at each point.

The data point with the least separation was considered as the best match point.

Affine Transformation Matching: At this step, it was found that the template and the data points may not exactly overlap due to tilt in the data points. Additionally, the template points were pinned at the lowest point. Therefore a six-parameter transformation was performed between the template and the data points so that the template can fit with the data points.

$$a_1 x_t + a_2 z_t + a_3 = x_d$$
$$a_4 x_t + a_5 z_t + a_6 = z_d \qquad \text{(Eq. 1)}$$

where

x_t and z_t = template points coordinates,
x_d and z_d = nearest girder points coordinates and
a_1 to a_6 = the affine transformation parameters.

This process was implemented to allow the template to rotate and shift to best fit the girder points. Fig. 7 shows the results after affine transformation where the template points are over the data points. The yellow color markers show the CMPs. The closest data point coordinates from the CMPs were recorded as profile points at low, mid and high points on the girder. These points were plotted to determine the girder deformation profile both vertically (Z-direction) and horizontally (Y- direction).

Results and Discussion

At this stage, results from the plane detection step and the template matching steps were available. The results are presented in this section.

Girder Deformation Detection – Using the plane equation, the points away from it were color coded to show different deformations within each panel and also between the columns. These results were shown in Figs. 5c and 5d. It can be noted from the results that deformation within a panel were not significant whereas deformations were significant between column-to-column color maps. Similar results were obtained for the remainder of the length of the data.

Profiles at the Low, Mid and Top Location of the Girder – The results from the template matching steps were plotted as graph to a plan view of the three profiles: low, mid and top along the face of the girder's web. A moving average filter was implemented to identify any outliers.

Fig. 8 shows the distances from the bay center to the girder's top, mid and low CMPs. It can be observed that the locations where the three points are not over each other shows a tilt in the girder's web. The trend of these profiles also shows the girder deviations from the centerline. Regions identified in Fig. 8 as A, B, C and D show that the girder is deviating closer to the bay (shown as A) centerline and away (shown as B, C and D) by more than few inches.

Conclusions

This paper described the methodology to model gantry crane girders for deformation monitoring. Two approaches were developed to analyze the girders. In the first approach, the surface variations of the girder were color coded to show changes in the surface variations. In the second approach, points on the surface of the girder were extracted at bottom, mid, and top locations, which showed its deformations within the panel and along the length of the girder. The results showed that the proposed methodology was able to determine girder deformations both at local and for the entire length.

The results presented in this paper showed that this methodology can determine deformations on the girder's surface. The time requirement to process the data in Matlab was significantly lower compared

Figure 7

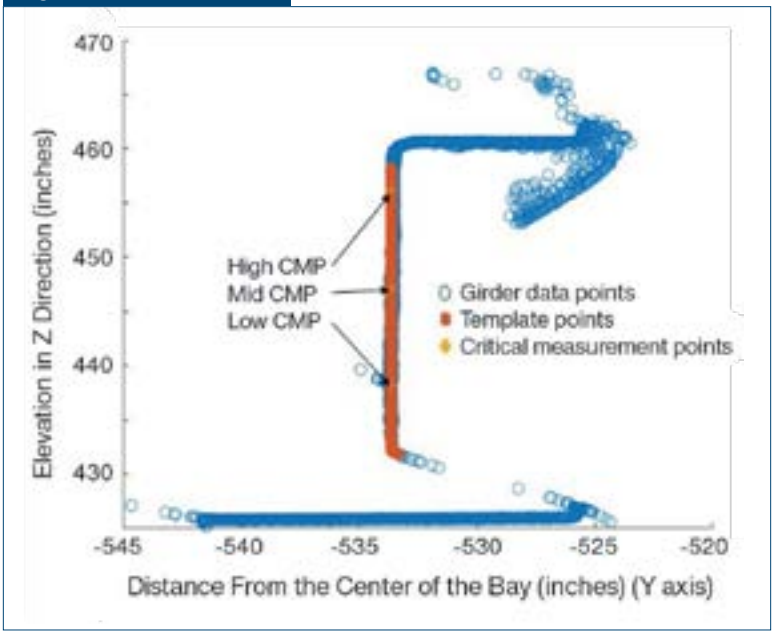

Results of point-to-point matching.

Figure 8

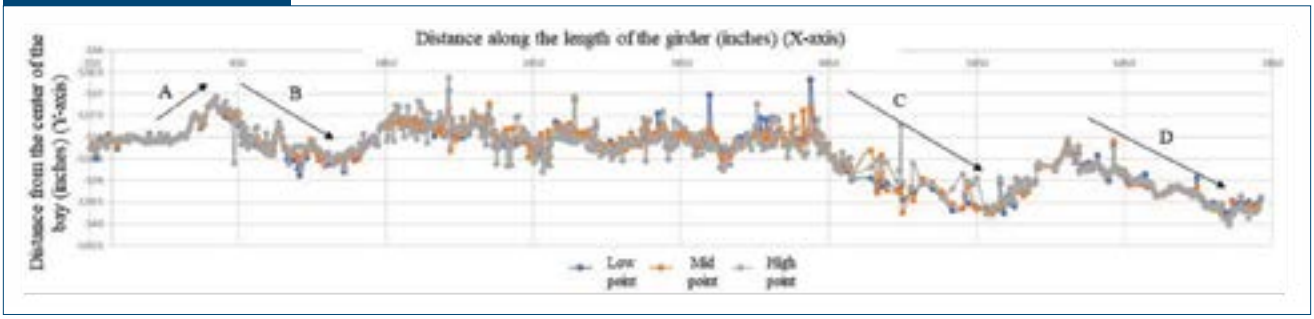

A top view of profiles showing distance from the bay center to the top, mid and low CMPs.

to manual analysis of data. Furthermore, minimum manual interaction results in an unbiased result free from human interpretation errors.

References

1. M. Falk, S. Deshpande, D. Zhang and N. Plooster, "Four-Dimensional Crane Rail Measurement," U.S. Patent US20210088407A1, 2021.
2. S. Deshpande, "Tunnel Modeling Using Mobile Mapping Lidar Points," American Society of Photogrammetry and Remote Sensing, 2021.
3. S.O. Elberink, K. Khoshelham, M. Arastounia and D.D. Benito, "Rail Track Detection and Modelling in Mobile Laser Scanner Data," *ISPRS Int. Arch. Photogramm. Remote Sens. Spat. Inf. Sci,* 2013, pp. 223–228.
4. M. Taheri Andani, A. Mohammed, A. Jain and M. Ahmadian, "Application of LIDAR Technology for Rail Surface Monitoring and Quality Indexing," *Proceedings of the Institution of Mechanical Engineers, Part F: Journal of Rail and Rapid Transit,* Vol. 232, No. 5, 2018, pp. 1398–1406.
5. M. Neubert, R. Hecht, C. Gedrange, M. Trommler, H. Herold, T. Krüger and F. Brimmer, "Extraction of Railroad Objects From Very High Resolution Helicopter-Borne LiDAR and Ortho-Image Data," *Int Arch Photogramm Remote Sens Spat Inf Sci,* Vol. 38, 2008, pp. 25–30.
6. S. Deshpande, M. Falk and N. Plooster, "Modeling Rollers Using Terrestrial Lidar Points in a Hot-Rolling Steel Mill," American Society of Photogrammetry and Remote Sensing, 2021.
7. J.K. Liu, R. Li, S. Deshpande, X. Niu and T.Y. Shih, "Estimation of Blufflines Using Topographic LiDAR Data and Orthoimages," *Photogrammetric Engineering & Remote Sensing,* Vol. 75, No. 1, 2009, pp. 69–79.
8. R. Li, S. Deshpande, X. Niu, F. Zhou, K. Di and B. Wu, "Geometric Integration of Aerial and High-Resolution Satellite Imagery and Application in Shoreline Mapping," *Marine geodesy,* Vol. 31, No. 3, 2008, pp. 143–159.
9. S. Deshpande, "Improved Floodplain Delineation Method Using High-Density LiDAR Data," *Computer-Aided Civil and Infrastructure Engineering,* Vol. 28, No. 1, 2013, pp. 68–79.
10. S. Deshpande and A. Yilmaz, "A Semi-Automated Method to Create a Lidar-Based Hydro-Flattened DEM," *International journal of remote sensing,* Vol. 38, No. 5, 2017, pp. 1365–1387.
11. M. Arastounia, "An Enhanced Algorithm for Concurrent Recognition of Rail Tracks and Power Cables From Terrestrial and Airborne Lidar Point Clouds," *Infrastructures,* Vol. 2, No. 2, 2017, p. 8.
12. S. Selvaraj and M. Madhavan, "Geometric Imperfection Measurements and Validations on Cold-Formed Steel Channels Using 3D Noncontact Laser Scanner," *Journal of Structural Engineering,* Vol. 144, No. 3, 2018, p. 04018010.
13. M. Cabaleiro, B. Riveiro, P. Arias and J.C. Caamaño, "Algorithm for Beam Deformation Modeling From LiDAR Data," *Measurement,* Vol. 76, 2015, pp. 20–31.
14. R.C. Gonzalez, R.E. Woods and S.L. Eddins, "Morphological Reconstruction," digital image processing using MATLAB, MathWorks, 2010. ✦

AISTech This paper was presented at AISTech 2021 — The Iron & Steel Technology Conference and Exposition, Nashville, Tenn., USA, and published in the AISTech 2021 Conference Proceedings.

Did You Know?

Swiss Steel Inks Hydropower Purchase Agreement

The Swiss Steel Group has reached a decarbonization milestone, switching its Steeltec special steel mill fully over to hydroelectric power.

According to the company, the Emmenbrücke, Switzerland, facility already had the lowest carbon intensity within the company, but the move to hydropower will lower it even further.

"We are proud today to be able to offer our customers steel melted exclusively with the use of Swiss hydro power," said Swiss Steel Group chief executive Frank Koch.

"We are thus making not only a decisive contribution to the decarbonization of our industry, but also to a greener, more sustainable society."

Swiss Steel is buying its power under a newly signed power purchase agreement with Swiss energy producer Axpo Holding. The agreement runs through 2024.